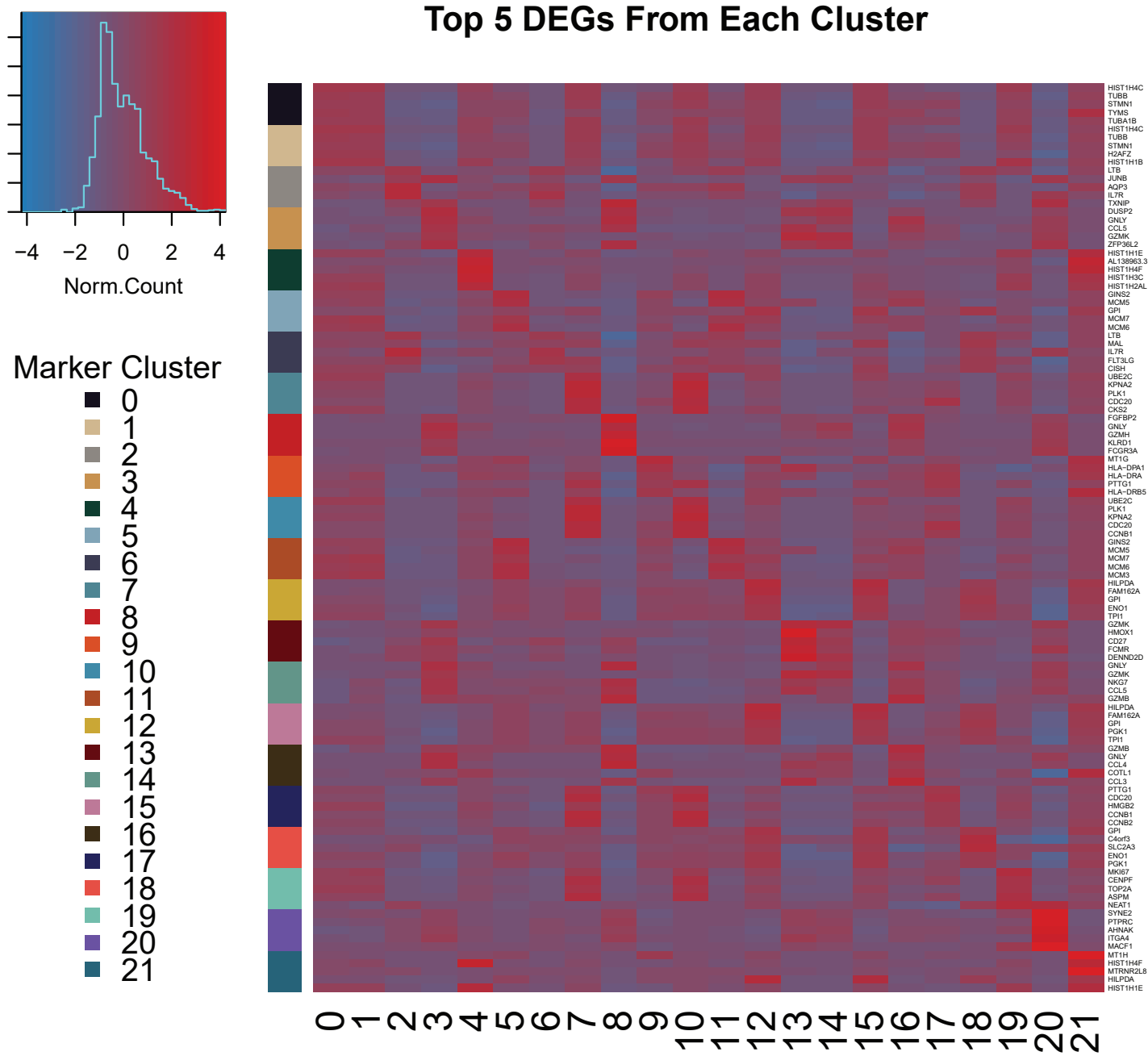
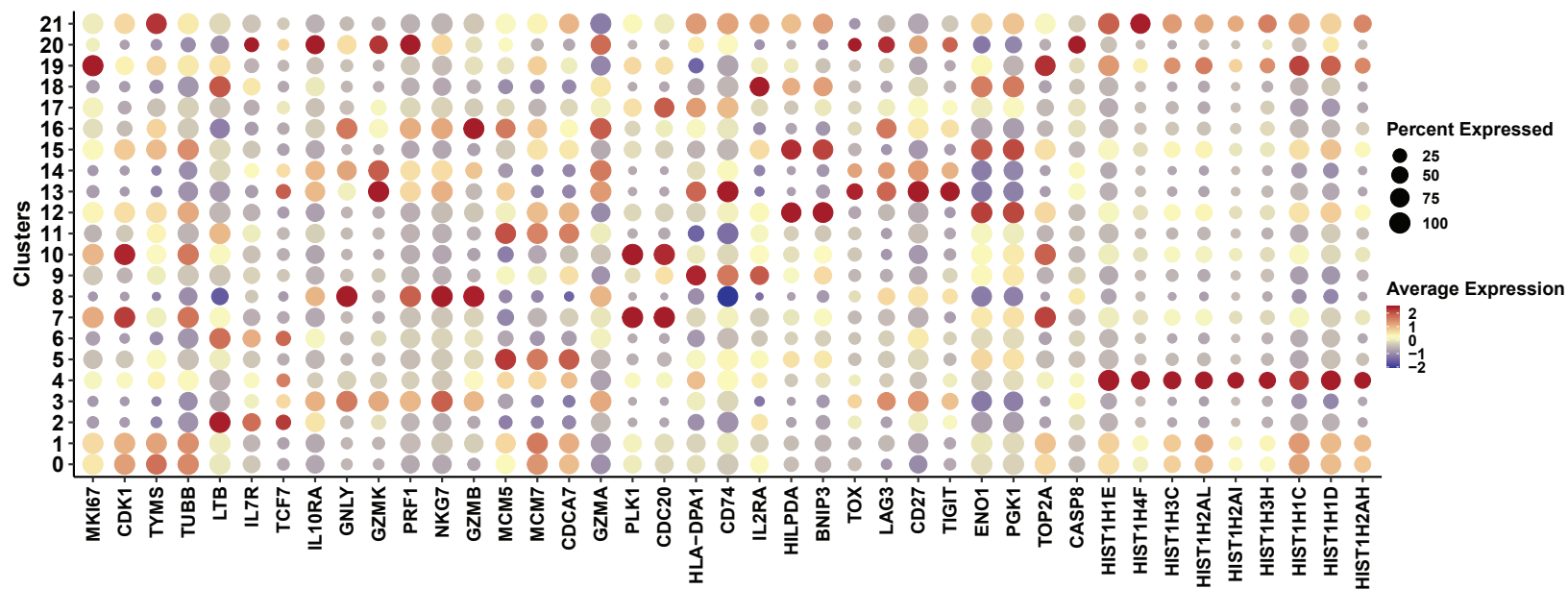


Figure S1

A

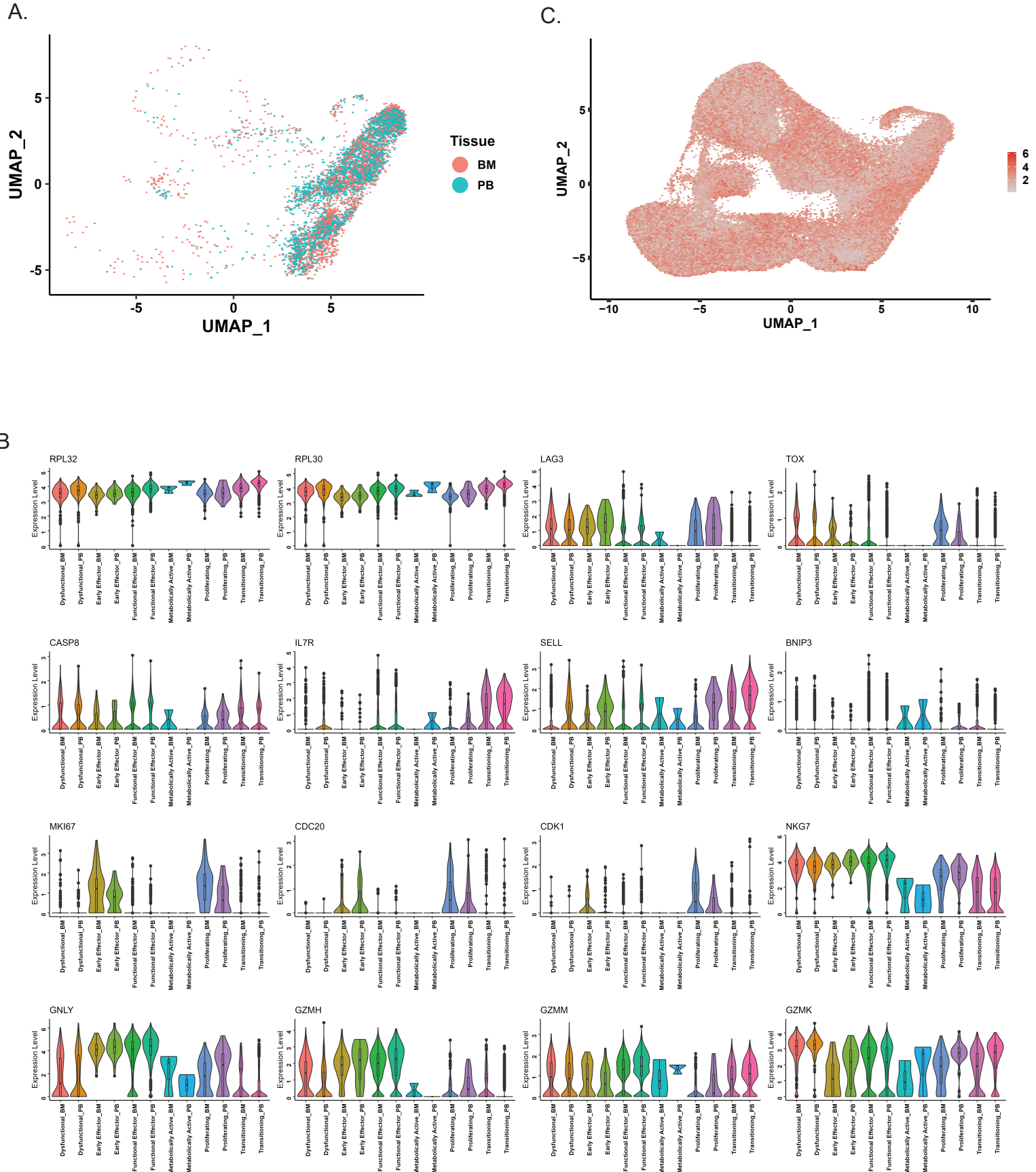


B



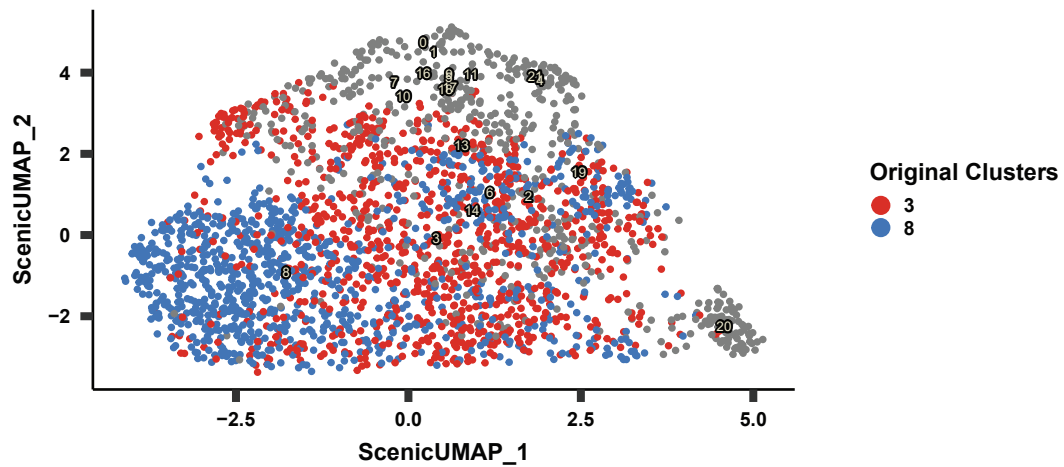
**Figure S1. Single cell transcriptomics of pre-and post-infusion CAR T cells.** **A**, Heatmap of the top 5 differentially expressed genes from each transcriptional cluster. **B**, Dot plot of relevant proliferation, T cell functional state, and histone-related genes.

Figure S2



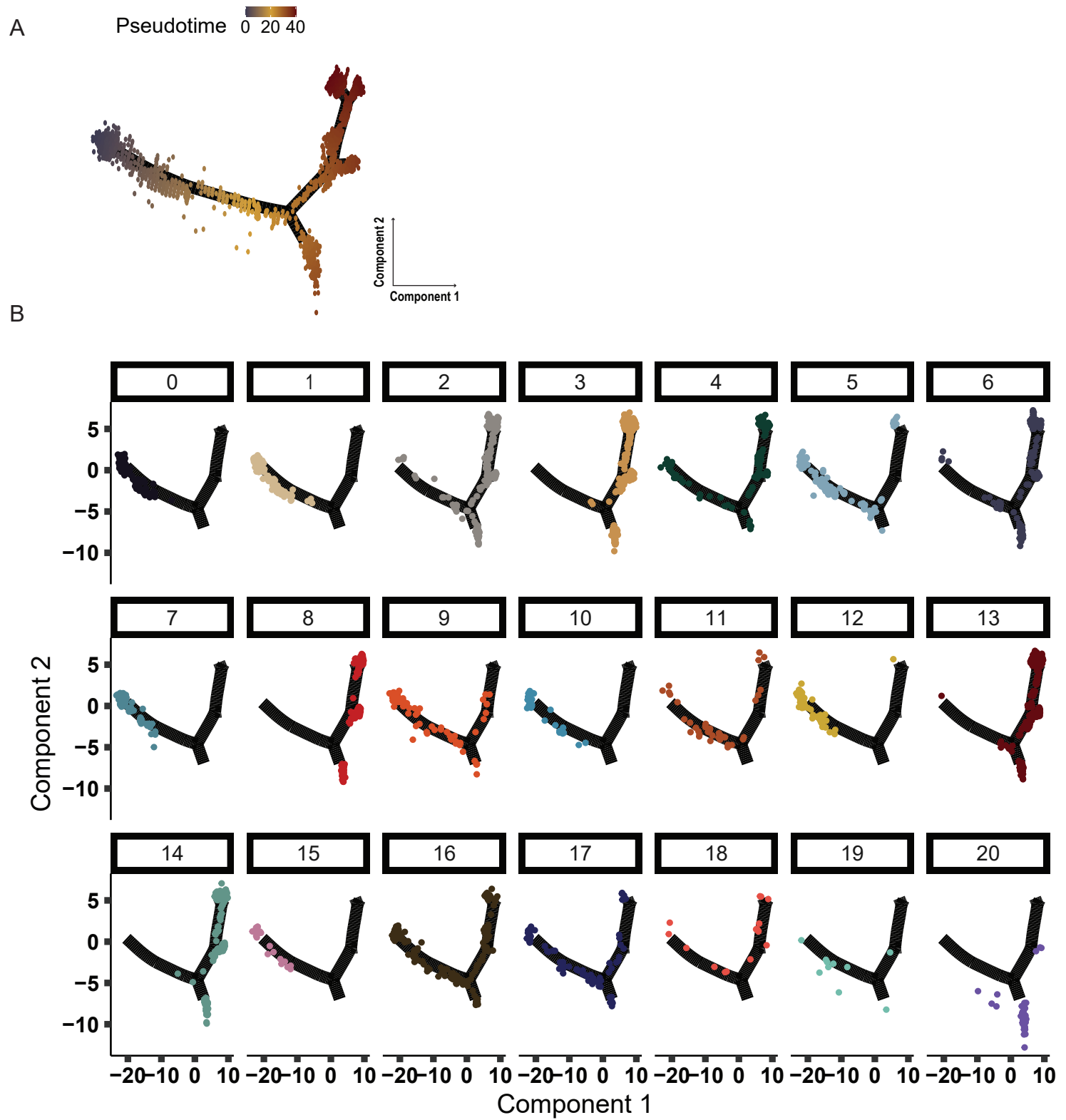
**Figure S2. Post-infusion peripheral blood and bone marrow CAR T cells have comparable transcriptional signatures.** **A**, UMAP of week 4 and month 4 post-infusion CAR T cells colored by sample type; bone marrow is colored in pink and peripheral blood is colored in blue. **B**, Violin plots comparing gene expression across peripheral blood (PB) and bone marrow (BM) CAR T cells from each functional group. **C**, UMAP of pre- and post-infusion CAR T cells colored by detected expression of CD19-CAR transcript.

Figure S3



**Figure S3. Clusters 3 and 8 exhibit distinct transcription factor regulatory networks.** UMAP of downsampled CAR T cells clustered by differences in transcription factor regulons. Cluster 3 cells are colored red, cluster 8 cells are colored blue, and all other clusters are colored gray.

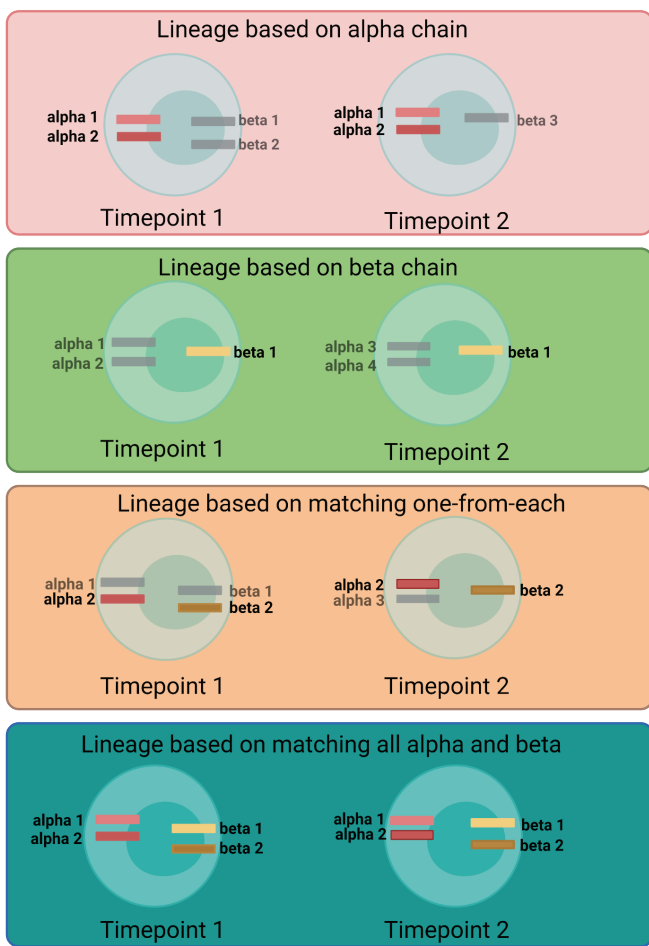
Figure S4



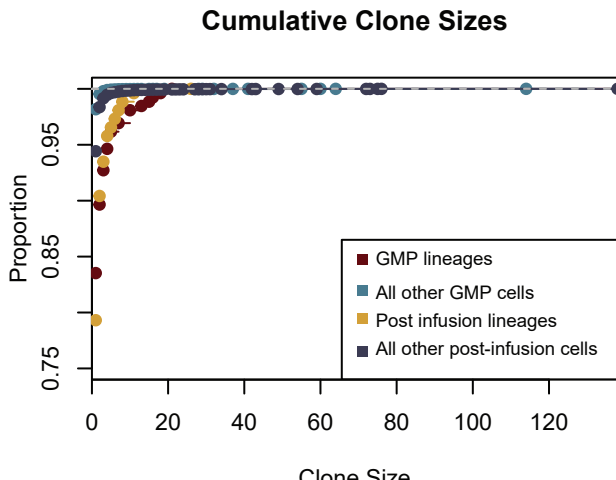
**Figure S4. Characterization of CAR T cells in pseudotime.** **A**, Monocle pseudotime map of CAR T cell transcriptional trajectory, colored by pseudotime gradient. **B**, Monocle pseudotime maps depicting each transcriptional cluster.

Figure S5

A

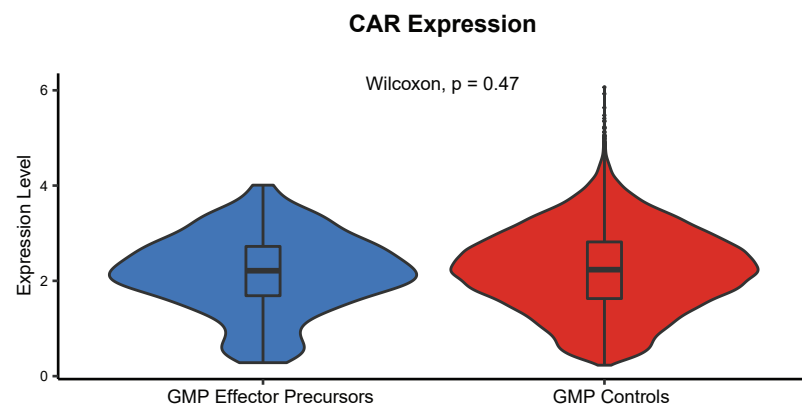


B



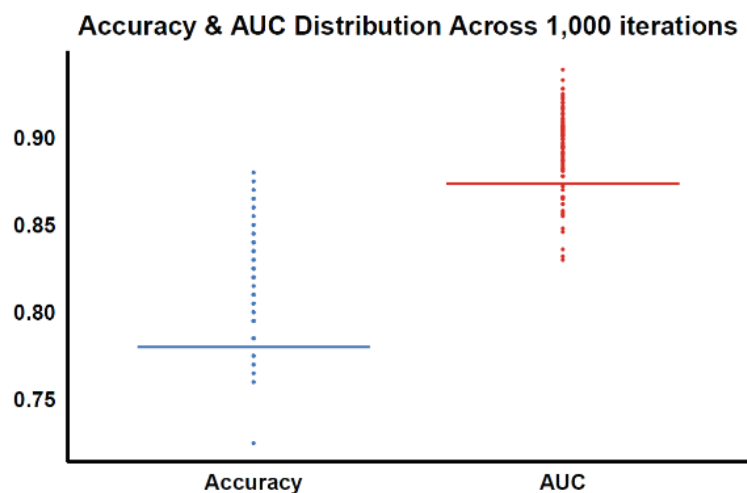
**Figure S5. TCR lineage tracking.** **A**, Different TCR  $\alpha$  and  $\beta$  matching schemes. The complementarity determining region 3 (CDR3) of each  $\alpha$  and  $\beta$  chain is sequenced to determine expressed alleles of each chain. Scheme 1 (red) describes classifying two CAR cells as in the same lineage when all observed  $\alpha$  alleles match exactly while disregarding the  $\beta$  chain. Scheme 2 (green) assigns cells to lineages based on complete matching in only the  $\beta$  chain. Neither scheme 1 nor 2 fully represents the TCR by neglecting the contribution of the other chain. Since cells can differentially express distinct alleles of both the  $\alpha$  and  $\beta$  chains of the TCR, the strictest definition of a lineage would be cases where all alphas and all betas must match between two or more cells (scheme 4; bottom). We detected the fewest number of lineages when requiring exact matches of all alleles (Supplementary Table 5). Thus, we defined lineages using a "one-from-each" approach (scheme 3; orange), where cells that match their most highly expressed (as a stringency filter)  $\alpha$  and  $\beta$  chains are designated as lineages. **B**, Cumulative clone sizes of: GMP (dark red) and post-infusion (yellow) CAR T cell lineages, and GMP (light blue) and post-infusion (dark blue) CAR T cells without observed lineages (all other GMP/post-infusion cells). Graph represents the proportion of cells (y-axis) cumulatively encompassed by increasing clone sizes.

Figure S6



**Figure S6. The distinct transcriptional signature between GMP effector precursors and non-precursors is not driven by differences in CAR expression.** Violin plots comparing CAR transcript expression level between effector precursors (blue) and non-precursors (red) in the GMP. Adjusted p-value = 1.

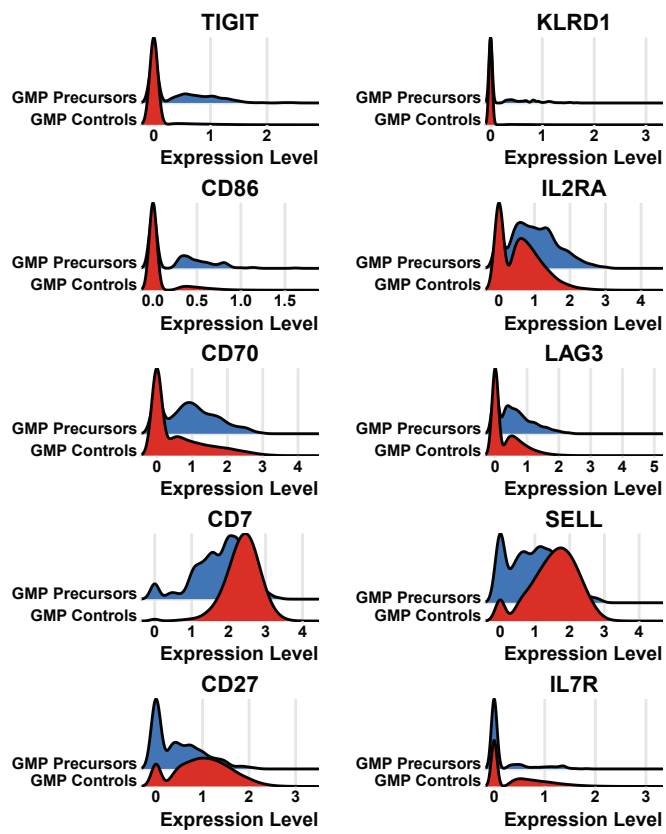
Figure S7



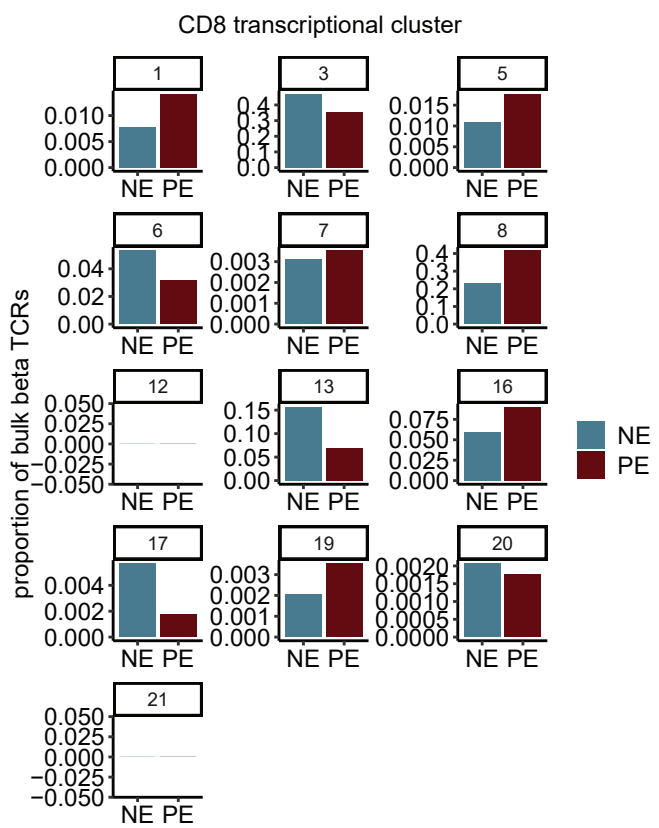
**Figure S7. Summary of repetitive iterations of effector precursor classifier performance.** Box plot summarizing the distributions of both the accuracy and the AUC across all 1,000 iterations. The box plot was graphed to show the median, upper and lower hinges (25th and 75th percentiles), two whiskers ( $1.5 \times \text{IQR}$ ), and all outlier points (points  $> 1.5 \times \text{IQR}$ ).

Figure S8

A



B

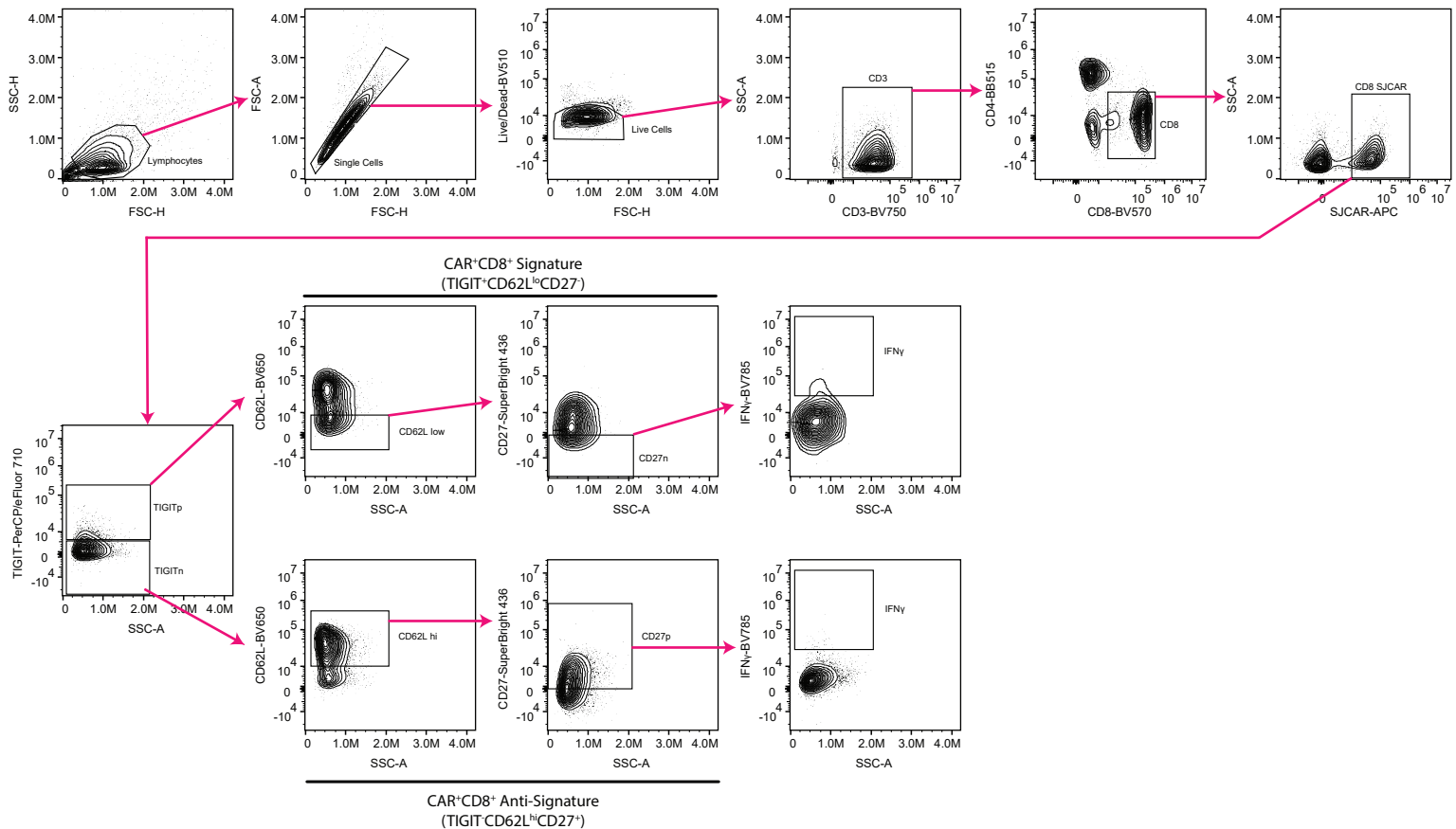


**Figure S8. Selection of surface targets for pre-effector CAR T cell surface phenotype validation and results of enrichment.** **A**, Histograms comparing expression of a subset of genes encoding surface proteins in effector precursors (blue) and non-effector precursors (red). **B**, Bar plots representing the inferred proportions of post-infusion CD8 transcriptional clusters linked to Patient 11 GMP CAR T cells sorted to approximate either the pre-effector signature (PE) or the opposing, non-effector signature (NE). TCR $\beta$  chains were sequenced in bulk from each sort, and cluster-annotated post-infusion cells from CD8 clusters that shared those  $\beta$  sequences were used to infer the post-infusion transcriptional cluster those lineages would track to.

Figure S9

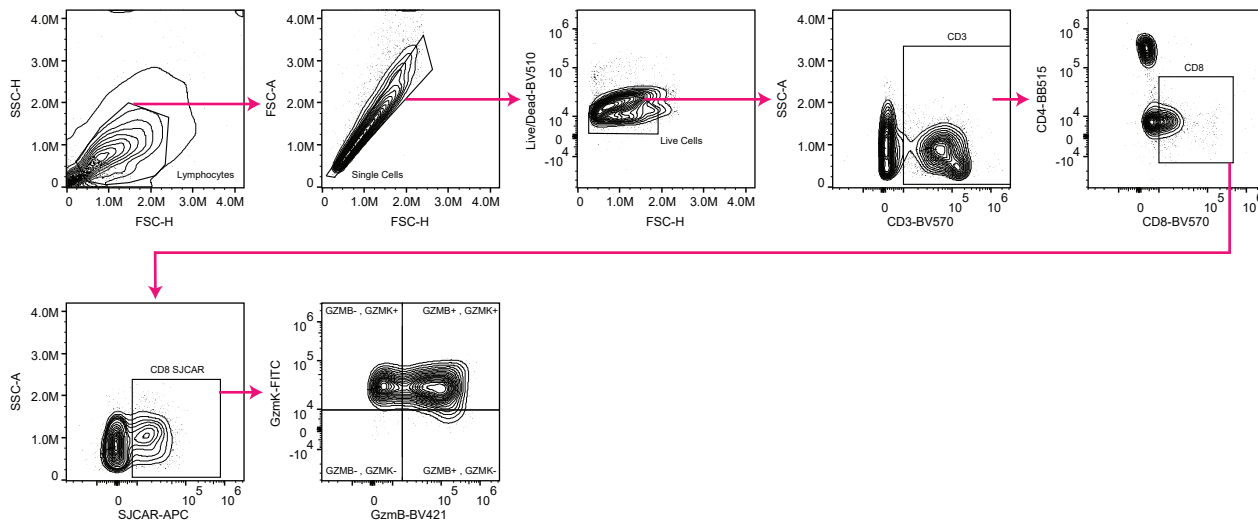
A

Pre-infusion (GMP)



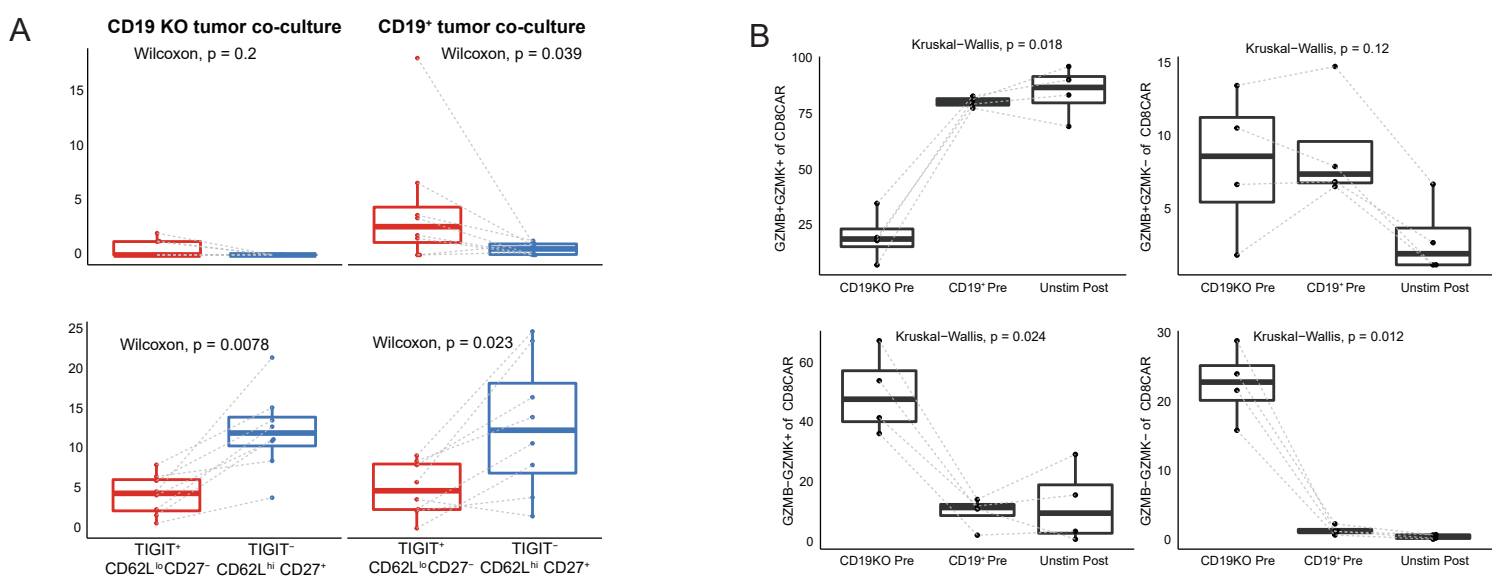
B

Post-infusion (Patient Collection)



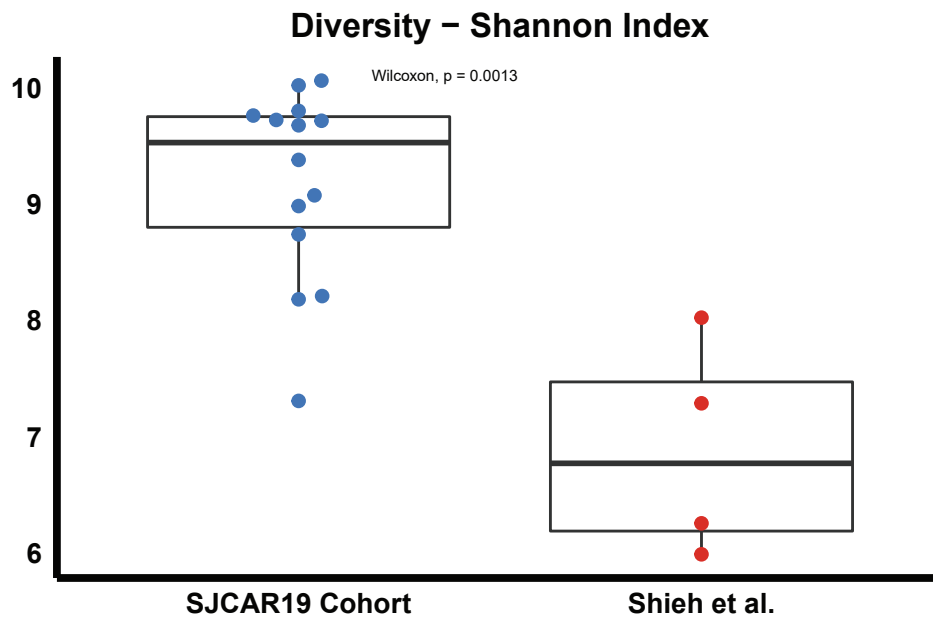
**Figure S9: Flow cytometry gating strategies for surface phenotyping and intracellular cytokine staining of SJCAR19 GMP and post-infusion samples. All samples were gated on lymphocyte-sized, single, live, CD3+, CD4-, CD8+, CAR+ cells.** **A**, Gating strategy applied to GMP (pre-infusion) samples to evaluate IFNy production from the CD8+CAR+ signature (TIGIT+, CD62Llo, CD27-) and CD8+CAR+ anti-signature (TIGIT-, CD62Llo, +CD27+) lymphocytes. **B**, Gating strategy applied to post-infusion samples to assess frequencies of TOX and IFNy-producing cells across CD8+ CAR T cells with differential staining of GzmB and GzmK. IFNy (interferon gamma); TIGIT (T Cell Immunoreceptor with Ig and ITIM Domains); GzmB (granzyme B); GzmK (granzyme K); TOX (Thymocyte Selection Associated High Mobility Group Box); CCR5 (C-C Motif Chemokine Receptor 5); CX3CR1 (C-X3-C Motif Chemokine Receptor 1). Gating strategy prepared using FlowJo v10.7.1 software (TreeStar).

Figure S10



**Figure S10. Flow cytometry data from validation patient cohort.** **A**, Box plots comparing the percent of IFN $\gamma$ -producing CD8+ CAR T cells (top) and TOX-producing CD8+ CAR T cells (bottom) between effector precursor pre-infusion cells (Tigit+, CD62L<sup>lo</sup>, CD27-; red) and pre-infusion cells with the opposing surface phenotype (Tigit-, CD62L<sup>hi</sup>, CD27+; blue) co-cultured either with CD19 KO tumor (left) or CD19+ tumor (right). Dashed lines pair individual patients across samples. Data is from GMP samples of patients not included in the initial transcriptional profiling dataset (patients 16-23). **B**, Box plots comparing the percent of GZMB+ GZMK+ (top left), GZMB+ GZMK- (top right), GZMB- GZMK+ (bottom left), and GZMB-GZMK- (bottom right) CD8+ CAR T cells across pre-infusion CAR T cells co-cultured with either CD19KO or CD19+ tumor and unstimulated post-infusion CAR T cells. Patients included in analysis are 16, 17, 22, and 23 from the validation cohort.

Figure S11



**Figure S11. GMP products generated from pediatric patients exhibit extreme clonal diversity compared to those generated from adult patients.** Box plots comparing the  $\beta$  chain diversity of CAR T cell TCRs from the GMP product in pediatric patients from the current study compared to those from adult patients in a previously published study (Sheih et al 2020, Nature Communications). The Shannon-Wiener index was calculated for each patient, and a Wilcoxon test was performed to evaluate statistical significance.